vol. 176, no. 1 the american naturalist july 2010 Ⓔ

E-Article

Spatial Self-Organization on Intertidal Mudflats through Biophysical Stress Divergence

Ellen J. Weerman,[1,2,*] Johan van de Koppel,[1] Maarten B. Eppinga,[3] Francesc Montserrat,[1,4] Quan-Xing Liu,[1] and Peter M. J. Herman[1]

1. Centre for Estuarine and Marine Ecology, Netherlands Institute of Ecology (NIOO-KNAW), P.O. Box 40, 4400 AC Yerseke, The Netherlands; 2. Aquatic Ecology and Ecotoxicology, Institute for Biodiversity and Ecosystem Dynamics, University of Amsterdam, P.O. Box 94240, 1090 GE Amsterdam, The Netherlands; 3. Department of Plant Biology, University of Vermont, Burlington, Vermont 05405; 4. Delft University of Technology, Faculty of Civil Engineering and Geosciences, Hydraulics Section, P.O. Box 5048, 2600 GA Delft, The Netherlands

Submitted September 4, 2009; Accepted January 8, 2010; Electronically published May 24, 2010

Online enhancement: video.

---

abstract: In this study, we investigated the emergence of spatial self-organized patterns on intertidal flats, resulting from the interaction between biological and geomorphological processes. Autocorrelation analysis of aerial photographs revealed that diatoms occur in regularly spaced patterns consisting of elevated hummocks alternating with water-filled hollows. Hummocks were characterized by high diatom content and a high sediment erosion threshold, while both were low in hollows. These results highlight the interaction between diatom growth and sedimentary processes as a potential mechanism for spatial patterning. Several alternative mechanisms could be excluded as important mechanisms in the formation of spatial patterns. We developed a spatially explicit mathematical model that revealed that scale-dependent interactions between sedimentation, diatom growth, and water redistribution explain the observed patterns. The model predicts that areas exhibiting spatially self-organized patterns have increased sediment accretion and diatom biomass compared with areas lacking spatial patterns, a prediction confirmed by empirical evidence. Our study on intertidal mudflats provides a simple but clear-cut example of how the interaction between biological and sedimentary processes, through the process of self-organization, induces spatial patterns at a landscape level.

Keywords: biogeomorphology, diatom, sediment, ecosystem functioning, Westerschelde, scale-dependent feedback mechanisms.

Introduction

In the past decade, a large number of studies have reported on regular pattern formation in a wide range of ecosystems (for a review, see Rietkerk and van de Koppel 2008). Theoretical studies proposed that regular pattern formation is induced by feedback mechanisms acting on different scales (Levin and Segel 1985). Here, facilitation processes locally improve living conditions through, for instance, the accumulation of nutrients (oligotrophic peatlands) or water (arid ecosystems), causing a small-scale positive feedback. This is countered by larger-scale inhibitory processes—for instance, through depletion of resources—that cause a negative feedback (Couteron and Lejeune 2001; Rietkerk et al. 2002, 2004*a*; Eppinga et al. 2008). This scale-dependent feedback mechanism can explain the formation of regular spatial patterns in many ecosystems and is predicted to have important implications for ecosystem functioning in terms of increased production or resilience (Rietkerk and van de Koppel 2008).

Theoretical studies have mainly focused on concentration of limiting resources when explaining regular pattern formation in ecosystems. However, field studies have pointed to possible alternative mechanisms for explaining regular patterns in ecosystems that are based on divergence of physical stresses, for example, the divergence of water flow or snow (Temmerman et al. 2005; Hiemstra et al. 2006; Larsen et al. 2007; van Wesenbeeck et al. 2008). On salt marshes, for instance, clumps of vegetation obstruct water flow, which locally improves growth conditions. Divergence of water flow around vegetation clumps increases erosion, which limits plant growth just outside the clump and hence induces a scale-dependent feedback. This mechanism has been suggested to trigger the development of spatial structure in salt marshes and even affect landscape formation in this ecosystem (D'Alpaos et al. 2007; Temmerman et al. 2007; van Wesenbeeck et al. 2008). Whether it can explain the formation of regular, self-organized spatial patterns has remained unstudied.

In this study, we describe how redistribution of hydrodynamic stress by diatoms can explain the formation of regular patterns on intertidal mudflats. Here, elevated

---

[*] Corresponding author; e-mail: e.weerman@nioo.knaw.nl.

Am. Nat. 2010. Vol. 176, pp. E15–E32. © 2010 by The University of Chicago. 0003-0147/2010/17601-51577$15.00. All rights reserved.
DOI: 10.1086/652991

hummocks, covered with diatoms, alternate with water-filled hollows with few diatoms (fig. 1). Spatial patterning on muddy intertidal flats has been observed in a number of studies (Blanchard et al. 2000; de Brouwer et al. 2000; Gouleau et al. 2000; Whitehouse et al. 2000; Lanuru et al. 2007). They range from banded patterns aligned parallel to the flow direction (ridge-runnel systems) in areas where tidal currents are high (Bassoullet et al. 2000; Blanchard et al. 2000; Le Hir et al. 2000; Whitehouse et al. 2000) to round-shaped patterns where water currents are lower (de Brouwer et al. 2000). The linear ridge-runnel patterns are present during all the seasons (Lanuru et al. 2007), while the round-shaped patterns are a seasonal phenomenon (de Brouwer et al. 2000). Here, a spatial pattern of elevated hummocks alternating with water-filled hollows develops from a homogeneous mudflat in early spring and disappears again in summer (de Brouwer et al. 2000). On top of the hummocks, diatoms accumulate, forming a visible brown biofilm, which in turn is strengthened by the excretion of extracellular polymeric substances (EPS; Neumann et al. 1970). EPS inhibits erosion by increasing sediment cohesion and decreasing bottom roughness (Paterson 1989; Sutherland et al. 1998*a*, 1998*b*), resulting in increased sedimentation of fine-grained particles (de Brouwer et al. 2000; Montserrat et al. 2009), which subsequently stimulate growth of diatoms (van de Koppel et al. 2001). In the hollows, water accumulates during low tide, which will inhibit the buildup of EPS, as EPS dissolves in the overlying water (Blanchard et al. 2000; Paterson et al. 2000). This in turn leads to increased vulnerability to erosion during inundation and subsequently leads to erosion of diatoms and sediment. The interaction between accumulation of sediment on the hummocks and drainage of water toward the hollows is hypothesized to generate a scale-dependent feedback of short-scale facilitation and larger-scale inhibition of diatom growth and was put forward as a possible explanation for the observed spatial patterning (Rietkerk and van de Koppel 2008). However, this putative stress divergence mechanism has been neither studied mathematically nor tested empirically. Confir-

Figure 1: Photograph of a spatial diatom-sediment pattern taken at the intertidal flat on the Kapellebank, The Netherlands.

mation of stress divergence as a mechanism for the formation of regular self-organized spatial patterns in ecosystems would broaden the conceptual basis of scale-dependent feedback as a structuring process in ecological systems.

Here, we investigated the hypothesis that pattern formation on intertidal mudflats results from spatial self-organization that is caused by scale-dependent feedback between diatom growth, sediment dynamics, and water drainage processes. We developed a mathematical model of this feedback interaction to study stress divergence as a mechanism for the observed spatial pattern and its effect on the functioning of intertidal flats ecosystems. Aerial photographs were analyzed to establish the regularity of spatial patterns observed in the field. Subsequently, we investigated whether diatom biomass and sediment characteristics varied between the hummocks and the hollows to verify model assumptions and to exclude possible alternative mechanisms that could explain the observed spatial patterns. We furthermore tested in the field the model's prediction that patterned tidal flats accumulate more sediment and are more productive than homogeneous flats. This would solidify the concept that self-organized pattern formation affects ecosystem functioning.

A Simple Model of Pattern Formation on Intertidal Mudflats

Description

We developed a simple mathematical model to investigate whether the proposed scale-dependent feedback between diatom growth, sediment dynamics, and water drainage could result in regular spatial patterns on intertidal mudflats (fig. 1). Observations in the field revealed that the pattern is aligned parallel to the primary drainage direction of the intertidal mudflat. We therefore modeled a one-dimensional cross section of the intertidal mudflat aligned perpendicular to the drainage direction. The patterns in the field were dissected by larger drainage channels (app. B). We chose to ignore the large-scale drainage structure, since we were mostly interested in explaining the formation of patches. This simplifying approach allowed us to model small-scale pattern formation without explicitly taking into account large-scale hydrodynamic processes.

We modeled changes in sediment elevation (S; cm), water level (W; cm), and diatom biomass (D; g chlorophyll a m^{-2}) as a function of the interaction between diatom growth, sediment dynamics, and water flow from the hummocks toward the hollows. Diatom growth is described as the balance between growth and losses due to erosion by the overlaying water:

$$\frac{\partial D}{\partial t} = rD\left(1 - \frac{D}{k}\right) - ECD\frac{W}{q + W}. \tag{1}$$

Here, growth of diatoms is described using the logistic growth equation, where r is the intrinsic growth rate of the diatoms and k is the diatom carrying capacity. Furthermore, E is the maximal sediment erosion rate in the absence of diatoms, C translates sediment erosion to the rate of diatom losses, and q is the water level at which diatom losses are half maximal. Diatom losses by other processes—for example, grazing—are ignored since these are fairly low during development of spatial patterns early in the season.

Changes in sediment level are determined by the balance between deposition and erosion of sediment particles from the overlying water during tidal submergence. Deposition of sediment occurs each high tide as a small amount of sediment settles down from the water column. Erosion depends on diatom biomass since diatoms decrease erosion through the exudation of EPS (Paterson 1989; Sutherland et al. 1998*a*, 1998*b*):

$$\frac{\partial S}{\partial t} = S_{\text{in}} - E\left(\frac{k - Dp_{\text{E}}}{k}\right)S + A\frac{\partial^2 S}{\partial x^2}, \tag{2}$$

where S_{in} is the sediment deposition rate and p_{E} is the extent to which sediment erosion is reduced when diatoms are at carrying capacity. In the last term in the equation, A represents the diffusion constant describing slow, gravity-induced dispersion of wet sediment from the hummock to the hollows to avoid the generation of steep hummock edges.

In our model, changes in water level are determined by the residual amount of water left after each tide (W_{in}), the water drainage rate (F) in the direction perpendicular to our cross section, and the lateral flux of water:

$$\frac{\partial W}{\partial t} = W_{\text{in}}|WF + \frac{\partial}{\partial x}\left[K(W)W\frac{\partial (W + S)}{\partial x}\right]. \tag{3}$$

Lateral water flow is modeled as a function of water depth and slope of the water surface ($\partial(S + W)/\partial x$), roughly following the Manning formula for open-channel flow, except for assuming a linear relation between water flow and water surface slope. By doing this, we could avoid the complexity of the shallow-water equations and maintain a simple model. Hydraulic conductivity ($K(W)$) is assumed to be a decreasing function of the water level, reflecting the reduced water flow rate in very thin water layers:

$$K(W) = K_{\mathrm{W}} \frac{TW^4 + p_K}{TW^4 + 1}. \tag{4}$$

Here, K_{W} is the conductivity when the water level is high, T translates water level to conductivity, and p_K is the proportion of K_{W} to which $K(W)$ reduces when the water level on the sediment approaches zero.

The model provides a strongly simplified representation of biological, hydrological, and sedimentary processes on an intertidal mudflat. It simultaneously considers water drainage from the hummocks to the hollows occurring at low tide and sedimentation processes occurring at high tide. The specific erosion rate is expressed as a monotonic function of diatom biomass, integrating the more complex relation between tidal water flow rate and sediment erosion (Winterwerp and Van Kesteren 2004) over longer timescales. Simplifying these processes maintains a tractable model and allows us to explore the effects of scale-dependent feedback mechanisms between diatoms and sedimentary processes on intertidal mudflats without explicitly considering tidal changes in water level. In this way, we aim to follow a principle-seeking approach that provides general understanding of the implications of sediment-diatom-water interactions, rather than a precise description of sedimentary and hydrodynamic processes.

The complexity of the systems (1)–(4) was reduced by adopting a quasi–steady state approach with respect to diatom biomass, assuming that diatom densities equilibrate within each tidal cycle. This allowed us to express diatom biomass algebraically:

$$D = k - \left(1 - \frac{EC}{r}\frac{W}{q + W}\right). \tag{5}$$

Inserting equation (5) in equations (1) and (2) reduces the model to a system of two partial differential equations. All parameters were derived from data that were collected during this study at reference sites, from the literature, or by estimation if no data were available. Table A1 in appendix A gives more information on the parameters we have used in the model.

The development of the patterns was simulated numerically with forward Euler integration of the differential equations using Intel Visual Fortran. We simulated a vector of 600 points representing a length of 6 m perpendicular to the flow direction. Starting conditions were given by the homogeneous equilibrium, with a slightly evenly distributed random perturbation with a maximal difference of 0.006 cm. Periodic boundary conditions were adopted since the simulated domain was assumed to be a part of a larger intertidal bed. To avoid numerical instability, we used the harmonic mean of $K(W)$ from two neighboring points. Simulations were run until stability was reached.

Bifurcation Analysis

The occurrence of self-organized patterning is strongly affected by changes in biotic and abiotic conditions, and therefore we investigated how changes in key parameter values affected pattern formation and the predicted buildup of sediment and diatoms. To focus on the parameters that are essential to the model's behavior, we first derived a nondimensional version of the full model (app. A). The main factor of variation within and between intertidal flats is erosion, and therefore we investigated how changes in erosion rate affected pattern formation and the predicted buildup of sediment and diatoms. Other parameters from the nondimensional model were also studied and are described in appendix A. For the bifurcation analysis, we applied the method of spatial dynamics (Champneys 1996), which is an effective method for analyzing spatial steady state solutions (Sherratt and Lord 2007; Knobloch 2008; Wang et al. 2009). The analyses were performed using the bifurcation program AUTO (Doedel et al. 2001).

Results Model Analysis

Our model analysis shows that the interaction between diatom growth, sediment dynamics, and water drainage induces the development of regularly spaced, diatom-covered hummocks (fig. 2*A*, *green line*; see also video in the online edition of the *American Naturalist*). Pattern formation is initialized when a small, random increase in sediment elevation reduces the depth of the water layer and improves diatom growth, which in turn leads to a further increase in elevation. Water that accumulates in slightly lower parts causes the opposite effect as diatom losses increase, leading to more erosion and a further decrease of elevation. In the end, this results in a landscape of regularly placed hummocks with high diatom biomass on the hummocks, where water is drained toward the hollows in which water accumulated (fig. 2*B*). If the starting conditions are entirely homogeneous, no patterning develops, and both sediment elevation (fig. 2*A*, *dotted line*) and diatoms (fig. 2*B*, *dotted line*) remain low, revealing that spatial interactions are a key mechanism causing the formation of spatial patterns. This suggests that the proposed interaction between diatom growth, sedimentary processes, and water flow toward the hollows can explain the observed patterns on intertidal flats.

Bifurcation analyses revealed that the presence of spatial patterns was strongly dependent on parameter settings. Figure 3 presents the result of a bifurcation analysis for

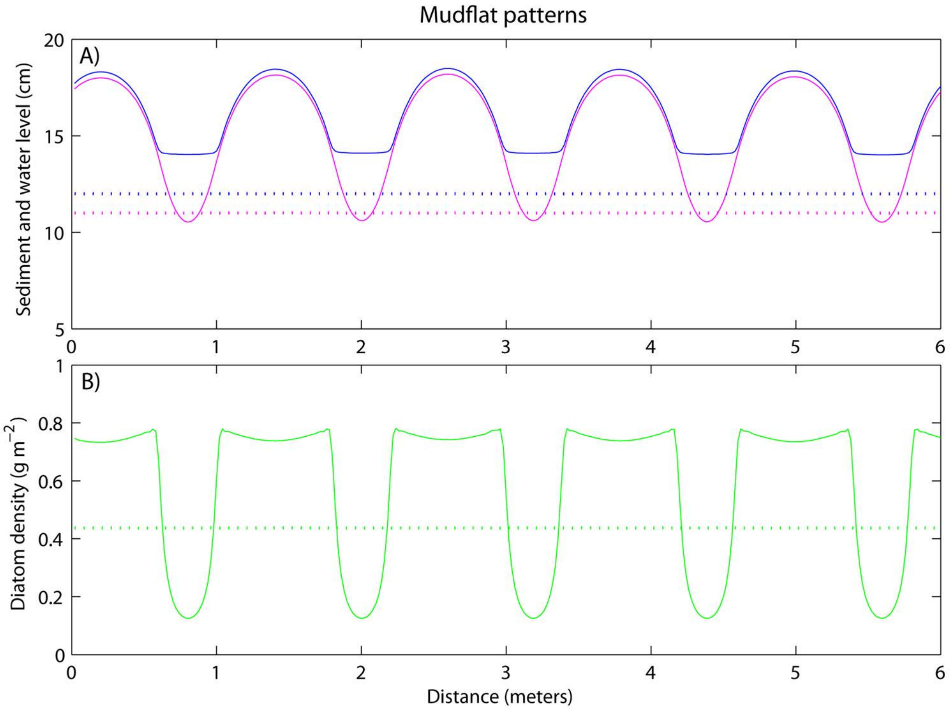

Figure 2: Simulated spatial patterns of sediment (*solid red line*), water level (*solid blue line*), and diatom biomass (*solid green line*) and the simulated homogeneous equilibrium for sediment (*dotted red line*), water level (*dotted blue line*), and diatom biomass (*dotted green line*). Parameters used as in appendix B. This figure is also available as a model simulation (QuickTime video, 1.94 MB) simulating the emergence of spatial patterns from small random differences in sediment bed level.

changes in the erosion rate E, which is the parameter that most clearly defines differences between intertidal habitats. In the homogeneous equilibrium, sediment level and diatom biomass decrease linearly with increasing erosion rate until diatoms cannot maintain themselves on the intertidal mudflat. This homogeneous equilibrium is unstable to small heterogeneous perturbations when $E > \mathrm{T}_2$. Here, small perturbations are inflated and cause the formation of regular spatial patterns (fig. 3, *solid blue line*). The patterned system is globally stable up to erosion rates of $E = \mathrm{T}_1$. Within $\mathrm{T}_1 < E < \mathrm{LP}_1$, the system has two attracting states, where one state is characterized by spatial patterns (*solid blue line*; represents maximal algal biomass or sediment levels in the patterned solution), while the other is a homogeneous state with few diatoms (*dashed black line*). Beyond a last threshold, the patterned state becomes unstable, and only a homogeneous state without diatoms is found ($E > \mathrm{LP}_1$; *solid black line*). The bifurcation analyses with respect to other parameters reveal qualitatively similar patterns. Pattern formation was found to be most sensitive to changes in the effects of diatoms on sediment erosion (app. A).

Our model allows us to investigate the implications of spatial pattern formation on ecosystem functioning. For all parameter values where stable patterns are predicted, average diatom biomass and sediment level are higher in the patterned equilibrium compared with the homogeneous equilibrium (fig. 3, *green lines vs. black lines*). Hence, in the patterned state, the intertidal mudflat is predicted to be more productive and accumulate more sediment compared with a homogeneous intertidal mudflat, revealing that spatial patterning has important emergent effects on the functioning of intertidal mudflats that exceed beyond simple generation of heterogeneity and emphasizing the importance of diatom-induced spatial patterns for productivity and sediment capture on intertidal mudflats.

Testing Model Assumptions and Predictions

Description and Field Site

We conducted a field study to test a number of the assumptions and predictions of the model described in "A Simple Model of Pattern Formation on Intertidal Mudflats." First, we investigated, using aerial photographs, whether the observed patterns were indeed regular, as predicted by the model. Second, we investigated the differences in chlorophyll *a* content (a proxy for diatom biomass), sediment erosion thresholds, and sediment characteristics between the hummocks and the hollows. This was done to test the assumptions that underlie the model and to exclude possible alternative mechanisms for the observed spatial patterns. The model analysis identifies two important predictions: (1) self-organized patterns develop even in the absence of underlying environmental heterogeneity and (2) both diatom biomass and sediment accumulation at the scale of the tidal flat ecosystem (e.g., averaged over extensive areas) are higher in the patterned state compared with the homogeneous mudflat state. All experiments and measurements were done on the Kapellebank, an intertidal mudflat situated along the edges of the Westerschelde, The Netherlands (coordinates: 51.458521°N, 3.971685°E; fig. 1). Spatial patterns are abundant on approximately 75% of the total surface of the intertidal mudflat; they develop each year in spring and disappear at the onset of summer when benthic herbivore abundance increases.

Material and Methods

Pattern Observations

We analyzed aerial photographs of spatial patterns to test whether the observed patterns are regular. Aerial photographs were taken with a digital camera (Sony Cybershot DSC-V3) attached to a helium-inflated, blimp-shaped balloon (http://www.floatograph.com), which was attached to a tether line. Photographs were obtained from approximately 50 m height, covering an area of approximately 50 m × 40 m (3,072 pixels × 2,304 pixels; app. B). Generally, two types of patterns were detected on the Kapellebank: banded elongated patterns aligned parallel to the flow direction at the sloping sides of the mudflat, and more rounded patterns on the top of the intertidal flat where the slope is less pronounced. From both pattern types, two subsections of 300 pixels × 300 pixels (5 m × 5 m) were selected randomly for analysis, avoiding the larger drainage channels. In the extracted images, dark areas correspond to high diatom concentrations, and light areas correspond to bare sediment (fig. 4*A*, 4*D*). Visual inspection showed that the intensity of the blue channel within the RGB images reflected diatom biomass most closely, and therefore these pixel values were used for subsequent analysis. From the images, 3,000 pixels were sampled randomly, since the 300 × 300-pixel images were too large to be analyzed entirely. We tested for the spatial autocorrelation by calculating Moran's *I* using R (http://www.R-project.org). High positive autocorrelation corresponds to more similar diatom biomass at a specific distance, while dissimilarity results in negative autocorrelation (Legendre and Legendre 1998). Since on the sloping sides patterns seemed aligned along the general direction of water drainage, we analyzed the images in two directions: parallel and perpendicular to the average direction of the flow, using categories of 90°.

Underlying Heterogeneity

Our model predicts that self-organized patterns could develop in the near absence of underlying heterogeneity, for example, even on flat sediment. We tested this hypothesis in the field by removing both underlying heterogeneity and benthic diatoms in 2 × 2-m plots, while spatial patterns and diatoms remained untouched in the control plots. We added two additional procedural control treatments. In the first, called diatom removal only, diatoms were scraped from the sediment. In the second, labeled hummock removal only, the sediment was flattened, and the slurry of diatoms that was removed a priori was returned on the experimental plot. This block of four treatments was repeated 10 times following a randomized block design (Sokal and Rohlf 1995). The degree of recovery was determined after 14 days and expressed as the maximal elevation difference on the plot. A detailed description of this experiment is described in appendix B.

Testing for Model Assumptions

A crucial assumption for the proposed scale-dependent feedback mechanism is that erosion rates are high in the water-covered hollows compared with the emerged hummocks. In the field, we tested this assumption by determining the differences in diatom biomass, sediment properties, and the sensitivity of the sediment to erosion between the hummocks and the hollows. Therefore, chlorophyll *a*, silt content, and erosion threshold were measured at hummocks and adjacent hollows. A detailed description of these measurements is described in appendix A.

The mathematical model predicts higher sediment accretion and diatom biomass for a self-organized patterned intertidal flat compared with a homogeneous intertidal flat. We tested these model predictions in the field by measuring sediment accretion in plots where spatial patterns were present and in plots where spatial patterns were absent. Sediment bed level measurements were done in April 2009, when patterns were visible, and June 2009, when patterns had disappeared and the homogeneous bed level was stable, using the sediment erosion bar (SEB) method (Austen et al. 1999). We measured chlorophyll *a* content in April in both the spatially patterned plots and

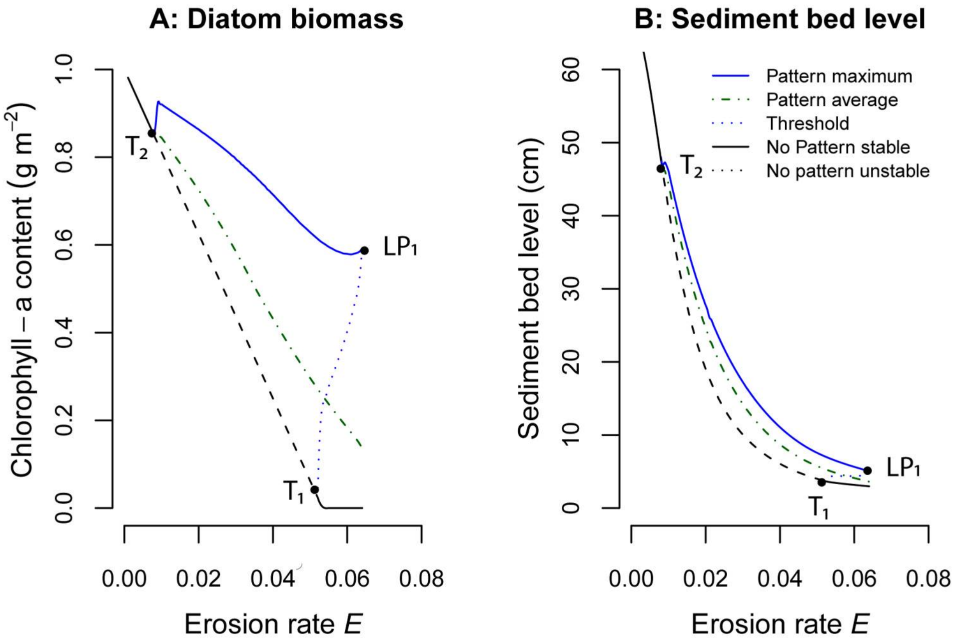

Figure 3: Bifurcation diagram of diatom biomass (*A*) and sediment accumulation (*B*) based on a single-peak solution. Black lines represent the homogeneous equilibrium, blue lines represent maximum diatom biomass in the patterned equilibrium, and green lines represent average diatom biomass of the whole domain in the patterned equilibrium. Solid and dotted lines represent the stable and unstable equilibria, respectively. T$_1$ ($E = 0.039$) and T$_2$ ($E = 0.012$) are Turing instability points, and LP$_1$ ($E = 0.0505$) is a limit point.

the homogeneous plots. A detailed description of these measurements is given in appendix A.

Statistical Analysis

Biotic and abiotic differences between hummocks and adjacent hollows were analyzed using Student's paired *t*-tests (one-tailed). To further analyze the influence of silt and chlorophyll *a* content on the variability in the erosion threshold for hummocks and hollows, we used a general linear model (GLM) with landscape position (hummock or hollows) as a fixed factor and silt content and chlorophyll *a* content as covariates. Using stepwise reduction from the saturated model (Crawley 2005), all nonsignificant factors could be removed, resulting in the best model for explaining differences in erosion threshold. Similarly, a GLM was used to analyze erosion threshold differences as a function of physical characteristics. The influence of spatial patterns on sediment accretion and chlorophyll *a* content were analyzed using Student's paired *t*-tests (one-tailed), testing the increase in elevation between April and June. All statistics were computed using R (http://www.R-project.org).

Results

Pattern Observation Data and Measurements

Spatial analysis of the aerial photographs revealed regular spatial patterning in diatom reflectance that was strongest perpendicular to the tidal flow direction. Patterns closer to the shoreline showed significant positive autocorrelation up to 20-cm lag distance, followed by significant negative autocorrelation from 20 to 80 cm (fig. 4*C*). This relation was not repeated in the flow direction, where autocorrelation was significantly positive up to 1.5-m distance (fig. 4*B*), but no negative correlation was found at any distance. This confirms that bands of high diatom biomass were regularly distributed in the direction perpendicular to the flow direction with a wavelength of roughly 1 m. The round-shaped patterns on the top of the intertidal mudflat revealed a similar relation (fig. 4*E*, 4*F*); these patterns were found to be regular in the direction perpendicular to the tidal flow direction, but no significant negative autocorrelation was observed in the opposite direction (0°), indicating the absence of regularity in this direction. Hence, we found regular patterning on both the sloping sides and the more flat top of the intertidal mudflat, mainly orientated perpendicular to the general direction of water drainage.

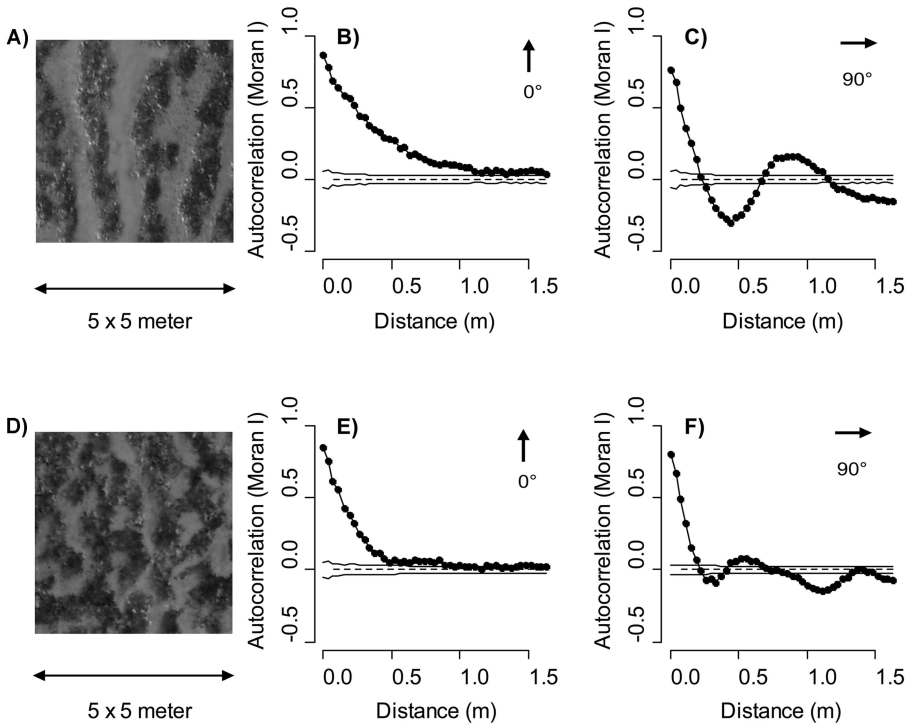

Figure 4: Autocorrelation (Moran's *I*) for benthic diatom patterns with their 95% confidence intervals (*gray lines*). Pictures represent a 5 × 5-m surface generated by two directional analyses, indicated by an arrow in the top right-hand corner. Two different patterns were chosen for this analysis: a banded pattern (*A*) and a more round-shaped pattern (*D*). Two directions correspond to 0° (*B*, *E*), which are parallel with the water line, and two correspond to 90° (*C*, *F*), perpendicular to the water line.

Analysis of the field measurements revealed that, in agreement with our hypothesis, higher chlorophyll *a* content ($P < .01$; fig. 5*A*) and higher erosion thresholds ($P < .001$; fig. 5*B*) were found on the hummocks compared with in the hollows. No significant differences in silt content were found (mean ± SEM: hummocks, 59.4% ± 2.3%, $P > .05$; hollows, 57.5% ± 2.9%, $P = .05$), indicating that variation in silt content was not the most important factor in determining the patchiness. Differences in chlorophyll *a* concentration and erosion threshold were to a large part explained by position on either hummocks or hollows. The GLM analysis revealed a model in which the factor landscape (e.g., in a hollow or on a hummock) gave the best fit (on the basis of Akaike information criteria) to measured erosion thresholds compared with models that included chlorophyll *a* and silt content and their interaction. Stepwise reduction from the saturated model (Crawley 2005), removing any nonsignificant factors, resulted in a model with only landscape position as the explanatory variable ($P < .001$). This is probably caused by a strong correlation between landscape position and chlorophyll *a* content, combined with limited variability of chlorophyll *a* content within either the hollows or the hummocks.

We found a strong effect of spatial patterns on sediment accretion during the spring season. Sediment bed level in patterned plots increased by 2.02 ± 0.31 cm (mean ± SEM), which is significantly higher than in homogeneous plots, which increased by 0.71 ± 0.76 cm ($P < .05$; fig. 6). Likewise, chlorophyll *a* was significantly higher in spatially patterned plots compared with homogeneous plots (135.61 ± 2.04 and 81.38 ± 10.74 $\mu g\ g^{-1}$; $P < .01$; fig. 6). Hence, these results support the prediction of our mathematical model that self-organized spatial patterns increase the overall sedimentation rate and diatom biomass.

Testing for Spatial Self-Organization

Experimental removal of heterogeneity did not affect the formation of hummock and hollows in the experimental plots. Two weeks after treatment application, no differences were found in bed level between control plots (3.12 ± 0.48 cm), treatment plots with hummock and diatom removal (2.50 ± 0.29 cm), or procedural controls

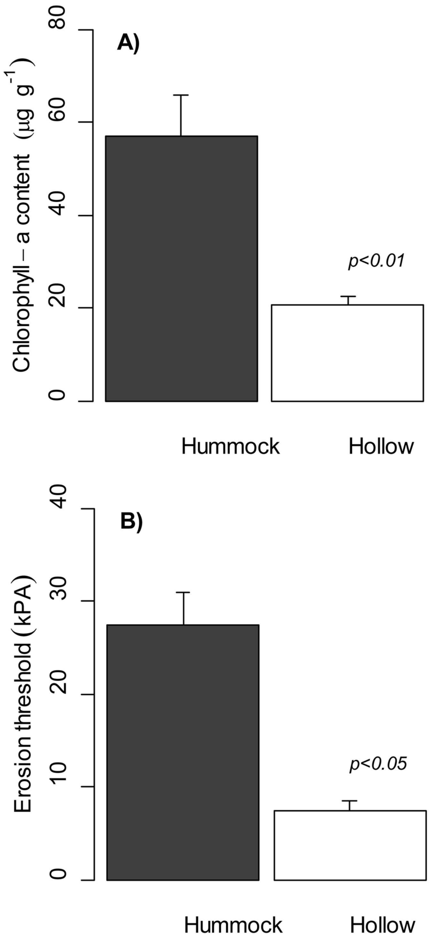

Figure 5: Differences in diatom biomass (*A*) and sediment stability (*B*) on the hummocks (*gray bars*) and hollows (*white bars*); $n = 7$, error bars denote ±1 SEM.

(diatom removal only: 2.82 ± 0.31 cm; hummock removal only: 2.58 ± 0.38 cm; fig. B2*A* in app. A; $P > .05$). Similarly, no differences in chlorophyll *a* content were measured on hummocks between the control plots (130.8 ± 10.8 µg g^{-1}), treatment plots with hummock and diatom removal (131.4 ± 13.81 µg g^{-1}), and procedural controls (diatom removal only: 127.26 ± 11.3 µg g^{-1}; hummock removal only: 136.3 ± 13.8 µg g^{-1}). Similarly, no differences in chlorophyll *a* content were found in the hollows (control plots: 51.7 ± 9.7 µg g^{-1}; treatment plots: 40.8 ± 8.0 µg g^{-1}) and procedural controls (diatom removal only: 44.3 ± 4.32 µg g^{-1}; hummock removal only: 48.2 ± 7.29 µg g^{-1}; fig. B2*B*; $P > .05$). This, in combination with the seasonal disappearance of patterning that was observed each year, makes it unlikely that underlying heterogeneity is a possible alternative mechanism for the formation of self-organized spatial patterns on intertidal flats.

Our results indicate that sediment consolidation, a possible alternative abiotic mechanism for pattern formation, did not differ between the hummocks and hollows. No differences were found for bulk density (1.21 ± 0.10 kg m^{-3} in hummocks vs. 1.13 ± 0.07 kg m^{-3} in hollows; $P > .05$). Similarly, no differences in water content were found between hummocks and hollows, as both showed 50% ± 3% water content. A GLM analysis, which included sediment consolidation variables as independent factors to explain differences in erosion threshold, identified that landscape position (e.g., hummock or hollow) was the main explanatory variable for the variation in erosion rate. Adding other factors such as bulk density and water content did not improve the explanatory power of the model.

Discussion

The formation of regular, self-organized spatial patterns has mainly been described in communities driven by resource limitation, where spatial redistribution of resources such as water or phosphate is the driving factor behind spatial self-organization (Rietkerk and van de Koppel 2008). This study presents an alternative mechanism for the formation of regular patterns: divergence of physical stress by organisms, creating local positive feedback but negative feedback at larger spatial scales. On intertidal mudflats, interactions between diatom growth and geomorphological processes locally improve living conditions for diatoms by increasing the elevation of diatom-covered hummocks. Consequently, increased elevation causes the hollows between hummocks to remain inundated at low water, decreasing diatom cover due to higher vulnerability to erosion and generating a scale-dependent feedback. Model analysis showed that this divergence of hydrodynamic stress induces a regular, self-organized spatial pattern on intertidal mudflats, resulting in a landscape of regularly spaced hummocks and hollows. Field measurements revealed a clear difference in both diatom biomass and erosion threshold between the hollows and the hummocks. This is in line with studies on other intertidal mudflats where regular patterning occurs (de Brouwer et al. 2000; Paterson et al. 2000; Lanuru et al. 2007). Furthermore, our model analyses as well as our experimental results reveal that self-organized patterns increased diatom densities and sediment capture, thereby increasing average elevation by about 2 cm. Hence, spatial pattern formation induced by stress divergence significantly affects the functioning of intertidal mudflat ecosystems.

Stress divergence mechanisms have been proposed in other studies to induce spatial structure in ecosystems (Hiemstra et al. 2002; Larsen et al. 2007; Saco et al. 2007; Temmerman et al. 2007; van Wesenbeeck et al. 2008). In

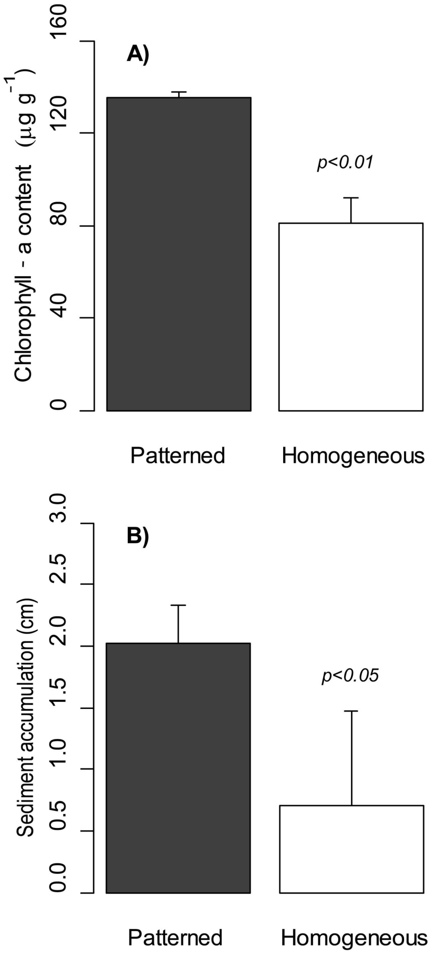

Figure 6: Diatom biomass (*A*) and sediment accretion (*B*) for the patterned stations (*gray bars*) and homogeneous stations (*white bars*). Diatom biomass is expressed as average chlorophyll *a* content, and sediment accretion is expressed as the difference in bed level between April and June; $n = 3$, error bars denote ± 1 SEM.

salt marsh ecosystems, tussocks of *Spartina anglica* improve growth conditions within the tussocks as a result of increased sedimentation but strongly decrease growth potential outside of the tussock. This mechanism induces the formation of creeks during salt marsh development (Temmerman et al. 2007). Stress divergence can be inferred from other studies in patterned ecosystems, such as during the formation of parallel tree lines in the Rocky Mountains (Hiemstra et al. 2006) or ridge and sloughs landscapes in the Everglades (Larsen et al. 2007). These studies, combined with ours, show that stress divergence might be a widely occurring mechanism causing spatial self-organization in ecosystems, broadening the application of spatial self-organization to a wider range of ecosystems.

Testing for Alternative Mechanisms

Our hypothesis that diatom-sediment interactions could explain the formation of the regular landscape of hummocks and hollows was tested against potential alternative mechanisms that could lead to spatial pattern formation. Possible alternative mechanisms include (1) underlying spatial heterogeneity, (2) increased sediment consolidation reducing sediment erosion on the hummocks, and (3) mechanical disturbance by water rushing through the hollows before submergence of the hummocks; these are all possible physical causes of patterning. We tested the effects of underlying heterogeneity by removing both diatoms and elevational differences in experimental plots. After 2 weeks, both diatom patterning and hummock development reappeared in these plots and were statistically indistinguishable from the control plots. This suggests that the patterns, at least in our experimental plots, are not the result of underlying heterogeneity. We did not observe differences in sediment bulk density or water content between the hummocks and the hollows, typical characteristics of consolidation. These results indicate that consolidation could not explain the observed differences in the sediment erosion threshold, and the diatom-sediment interactions are a more likely cause of the observed spatial patterns. Finally, two lines of reasoning point out that increased mechanical disturbance by water flow alone cannot explain the observed patterns. First, mechanical disturbance would lead to increased erosion in any low location and hence cannot explain the observed regularity. Second, water velocity has been found to be higher on hummocks compared with hollows (Williams et al. 2008), which would result in higher erosion on hummocks, which is opposite of what we found. This leads us to conclude that mechanical disturbance alone is an unlikely mechanism for the observed spatial patterns.

The importance of diatoms in stabilizing the sediment has been well established in the literature (Stal 2009), which also includes studies on spatially patterned intertidal flats (Paterson et al. 2000; Lanuru et al. 2007). Removal of benthic algae using biocide can result in extensive sediment erosion, affecting landscape formation (de Boer 1981; Underwood and Paterson 1993). These studies, in combination with other studies, point at the importance of diatom-sediment feedbacks in generating landscape heterogeneity (van de Koppel et al. 2001; Montserrat et al. 2008). Our own experiments suggest that stress divergence, caused by a local positive feedback between diatom growth and sediment accumulation, is the most likely cause of the observed regular patterns.

Biogeomorphological Feedback and Ecosystem Functioning

Our study reveals a clear effect of self-organized patterns on the functioning of intertidal mudflat ecosystems, since both the model and field data showed that patterned intertidal mudflats have significantly higher diatom densities and accumulation of sediment (fig. 6). The effect of this increase in diatom densities on overall intertidal mudflat productivity has hardly been investigated. Intertidal mudflats account for up to 50% of the primary production in estuaries (Underwood et al. 1999) and are therefore an important component of estuarine ecosystems. Increased benthic diatom biomass will significantly influence food availability, since diatoms are a major food source for benthic macrofauna (Herman et al. 2000; van Oevelen et al. 2006) and for the planktonic food web (de Jonge and van Beusekom 1992). Therefore, both benthic and planktonic faunal biomass is expected to increase with the presence of patterned intertidal mudflats within estuaries.

Our model analysis predicts increased sediment accumulation in self-organized intertidal mudflats. Although current models describing the morphology of intertidal mudflats have incorporated the effects of seasonal changes in diatom abundance on sediment surface texture (Paarlberg et al. 2005; Le Hir et al. 2007; Borsje et al. 2008), they lack the effects of self-organization induced by diatom-sediment feedbacks. Moreover, the increase in bed level can have important effects on water turbidity in the estuary on scales that far exceed that of a single intertidal mudflat. A back-of-the-envelope calculation reveals that 2 cm m^{-2} of diatom-induced accumulation of silt on an intertidal mudflat is roughly equivalent to the silt content of about 40 m^2 of open water (assuming an average depth of 10 m in the estuary; Herman et al. 2001). Similarly, benthic diatoms capture, although to a lesser extent, organic particulates from the water column, which can have a substantial effect on the particulate organic matter concentration within estuarine waters (Herman et al. 2001; Staats et al. 2001). In this way, self-organized spatial patterns not only locally affect the functioning of intertidal mudflats but also affect pelagic processes at the estuarine scale.

The bifurcation analysis uncovers two interesting possible implications of self-organization on patterned intertidal mudflats: the occurrence of alternative stable states and the vulnerability to catastrophic shifts. These implications limit our ability to predict how intertidal flats will respond to changes in forcing factors, such as increased flow rates, with respect to both sedimentary dynamics and their biological communities (van de Koppel et al. 2001). It is known that self-organized patterns may indicate the presence of alternative stable states and, as a consequence, a potential for catastrophic shifts, since both phenomena are, in part, the result of similar positive feedbacks (Scheffer and Carpenter 2003; Rietkerk et al. 2004*b*). On intertidal mudflats, this may result in sudden changes in diatom biomass and subsequent release of fine-grained sediment in response to gradually changing hydrodynamic conditions, which often are difficult to reverse. Addressing such nonlinear dynamics in estuarine systems will be an important future challenge in the study of biogeomorphology to provide more accurate predictions for management and conservation policies.

Our study emphasizes the need to integrate the fields of ecology and geomorphology to come to a general theory of the processes that underlie the formation of natural landscapes. So far, both fields have developed separate bodies of theory (Stallins 2006). Ecology has focused on the concept of spatial self-organization to explain pattern formation of vegetation and other organisms in homogeneous, flat landscapes (Rietkerk and van de Koppel 2008). Geomorphologists often use a static or linear description of the relation between organisms and physical processes to understand landscape formation, although the effects of vegetation on hydrodynamic and morphological processes are increasingly considered (Le Hir et al. 2000; Paarlberg et al. 2005; Hiemstra et al. 2006; Larsen et al. 2007; Saco et al. 2007; Temmerman et al. 2007; Borsje et al. 2008; van Wesenbeeck et al. 2008). Mudflat ecosystems provide a unique window on how integration of both fields can lead to detailed understanding of the importance of biogeomorphological interactions and the resulting spatial self-organization on the formation of natural landscapes.

Acknowledgments

We would like to thank J. Sherratt for help on the model analysis and K. den Hartogh for help in the field. We are also grateful to M. Rietkerk, B. R. Silliman, L. Stal, S. Temmerman, M. Vos, and two anonymous reviewers for valuable comments on earlier versions of this manuscript.

APPENDIX A

Model Parameters, Analysis, and Testing Model Assumptions

We present a table of the symbols, interpretation, units, values, and sources used in the model (table A1). Furthermore, we present the results of a detailed bifurcation analysis of equations (1)–(5) (“Model Analysis”) to focus on the parameters that are essential to the model’s behavior. We also present the detailed methods of the field measurements that were used for testing the model assumptions (“Testing for Model Assumptions”).

Table A1: Symbols, interpretation, units, values, and sources used in the model

Symbol	Interpretation	Unit	Value	Source
S_{in}	Sediment input	cm tide^{-1}	.2	Woods and Widdows 2002
E	Maximal erosion rate	tide^{-1}	.03	Estimated
p_{E}	Proportion of algae that erode	…	.90	Estimated
k	Carrying capacity of diatoms	g m^{-2}	1	E. J. Weerman, unpublished data
C	Maximum algal erosion	tide^{-1}	15	Estimated
r	Intrinsic growth rate diatoms	tide^{-1}	.4	Morris 2005
A	Diffusion factor lateral sediment transport	cm^2 t^{-1}	5	Estimated
q	Half-saturation constant diatoms	cm	.6	Estimated
F	Drainage factor	tide^{-1}	.2	Estimated
H_{in}	Water level left each tide	cm tide^{-1}	.2	Estimated
K_{W}	Conductivity when water level is high	cm t^{-1}	10	Estimated
p_K	Proportion of K_{W}	…	.1	Estimated
T	Translates water level to conductivity	…	200	Estimated

Model Analysis

Here, we present the results of a detailed bifurcation analysis of equations (1)–(5). To focus on the parameters that are essential to the model's behavior, we first derived a nondimensional model from the full model described in equations (1)–(3):

$$\frac{d\delta}{d\tau} = \delta(1-\delta) - \varepsilon\delta C\frac{\omega}{\gamma+\omega}, \tag{A1}$$

$$\frac{d\delta}{d\tau} = 1 - \varepsilon(1 - p_{\text{E}}\delta)\sigma - \frac{\partial^2\sigma}{\partial\psi^2}, \tag{A2}$$

$$\frac{\partial\omega}{\partial\tau} = 1 - \omega\phi + \frac{\delta}{\delta\psi}\left[K(\omega)\omega\frac{\partial}{\partial\psi}\left(\omega + \frac{S_{\text{in}}}{H_{\text{in}}}\sigma\right)\right]. \tag{A3}$$

Here $\delta = Dk^{-1}$, $\sigma = rSS_{\text{in}}^{-1}$, and $\omega = rWH_{\text{in}}^{-1}$. The spatial dimension is rescaled to $\psi = r^{1/2}A^{-1/2}X^{-1/2}$, and time is rescaled to the intrinsic growth rate of the diatoms ($t = r$). The model has seven rescaled parameters: $\varepsilon = Er^{-1}$, $\gamma = qrH_{\text{in}}^{-1}$, $\phi = Fr^{-1}$, $\kappa = K(W)H_{\text{in}}A^{-1}r^{-1}$, $\eta = S_{\text{in}}H_{\text{in}}^{-1}$, $\Lambda = C$, and $\rho = p_{\text{E}}$. From this nondimensional model, we have selected four parameters that were most directly related to habitat characteristics; for example, they would vary in space on tidal flats. These parameters were erosion rate (ε), the water level at which diatom losses is half maximal (γ), drainage factor (ϕ), and ρ, which describes to what extent sediment erosion is reduced when diatoms are in carrying capacity. For these four parameters, we conducted a bifurcation analysis using the bifurcation program AUTO (Doedel et al. 2001). We applied the method of spatial dynamics (Champneys 1996), which is an effective method in analyzing spatial steady state solutions (Sherratt and Lord 2007; Knobloch 2008; Wang et al. 2009). The bifurcation analysis shows that spatial patterns occur for a wide range of parameter values of the erosion rate E and drainage rate F (fig. A1, *gray area*). Pattern formation was found to be particularly sensitive to changes in the effects of diatoms on sediment erosion; pattern formation was observed only when p_{E} was larger than 0.5.

Testing for Model Assumptions

Here, we present the detailed methods of the field measurements that were used for testing the model assumptions. A crucial assumption for the model is that erosion rates are high in the water-covered hollows compared with the emerged hummocks. We tested this assumption by determining the differences in diatom biomass, sediment properties, and the sensitivity of the sediment to erosion between the hummocks and the hollows.

Material and Methods. Chlorophyll *a* content in the top layer of the sediment was used as a measure of diatom biomass, which is the main determinant of the EPS content in the sediment (Paterson et al. 2000) and was measured according to Jeffrey and Humphrey (1975). In April 2007, samples were taken in hollows and on adjacent hummocks during low tide. Surface sediment samples (top 2 mm, inner diameter 36 mm) were taken for chlorophyll *a* content using a cut-off syringe, and the samples were kept on ice during the fieldwork. Pigment extraction was done by adding 10 mL 90% acetone to extract the chlorophyll *a* content, after which this was analyzed using high performance liquid chromatography of the supernatant. Next to the chlorophyll *a* samples, sediment samples (top 10 mm, diameter 36 mm) for grain size and bulk density analysis were taken using a cut-off syringe. All samples were repeated sevenfold and were kept on ice during the fieldwork. In the laboratory, samples were weighed wet, freeze-dried, and weighed again. After this, the silt and clay content was determined as the fraction of the sediment that is smaller than 63 μm using laser diffraction (Malvern

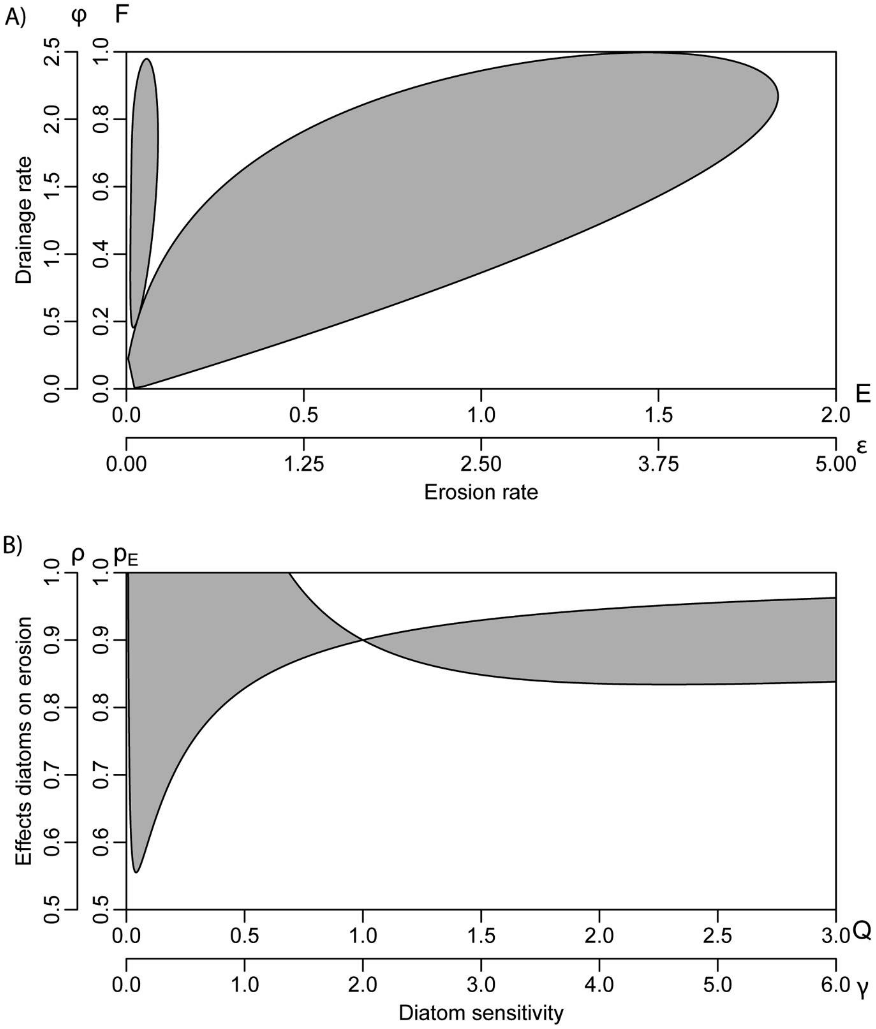

Figure A1: Bifurcation diagram of the sensitivity for changes in erosion rate and drainage factor on spatial patterns (*A*) and diatom sensitivity and diatom erosion on spatial patterns (*B*). Gray areas correspond to parameter values where spatial patterns are present, and white areas correspond to parameter values where spatial patterns are absent.

Particle Sizer 2000). We refer to this fraction as silt content in the rest of the article. Differences in sediment shear strength were quantified by using a cohesive strength meter, which provides a measure of the surface normal shear stress threshold beyond which sediment starts to erode, which we refer to as eroding threshold (Tolhurst et al. 1999, 2000). The eroding pressure values measured in this study should not be confused with horizontal bottom shear stress values reported in other studies. The methods that are in use express the eroding threshold in the same units (kPa) but differ in the way the pressure is imposed on the sediment and hence can lead to an order of magnitude difference in threshold values (Tolhurst et al. 1999).

The mathematical model predicts higher sediment accretion and diatom biomass for a self-organized patterned intertidal flat compared with a homogeneous intertidal flat. We tested these model predictions in the field where sediment accumulation was determined as the difference in bed level between April 2009, when patterns were visible, and June 2009, when the patterns had disappeared. The sediment bed level differences were compared between plots exhibiting spatial patterns ($n = 3$) and plots lacking clear spatial patterning ($n = 3$); both were present on the Kapellebank, The Netherlands. Bed level measurements were carried out using the sediment erosion bar method, adapted from Austen et al. (1999), where two metal poles of 200 cm length were pushed into the sediment at a distance of 1.5 m away from each other. During the measurements, a portable aluminum frame was placed on top, and the distance from this frame to the sediment was measured in between the poles at 11 points spaced 10 cm from each other with an accuracy of about 1 mm (van Wijnen and Bakker 2001). At each plot, chlorophyll *a* samples of the top 1 cm of the sediment were taken using a cut-off syringe (diameter 1 cm). In the laboratory, chlorophyll *a* samples were freeze-dried and analyzed spectrophotometrically after a 48-h extraction in 90% acetone (Jeffrey and Humphrey 1975). Sediment characteristics of these samples were determined as described above.

Statistical Analysis. Biotic and abiotic differences between hummocks and adjacent hollows were analyzed using Student's paired *t*-test (one-tailed). To further analyze the influence of silt and chlorophyll *a* content on the variability of erosion threshold of hummocks and hollows, we used a GLM with landscape position (hummock or hollows) as a fixed factor and silt content and chlorophyll *a* content as covariates. Using stepwise reduction from the saturated model (Crawley 2005), all nonsignificant factors could be removed, resulting in the best model explaining differences in erosion threshold. Similarly, a GLM was used to analyze erosion threshold differences by physical characteristics. The influence of spatial patterns on sediment accretion and chlorophyll *a* content was analyzed using Student's paired *t*-tests (one-tailed), testing the increase in elevation between April and June. All statistics were computed using R (http://www.R-project.org).

APPENDIX B

Spatial Patterns and the Effects of the Removal of Underlying Physical Heterogeneity on the Formation of Spatial Patterns

Here, we present the detailed methods and results of a manipulative field experiment in which we tested the ef-

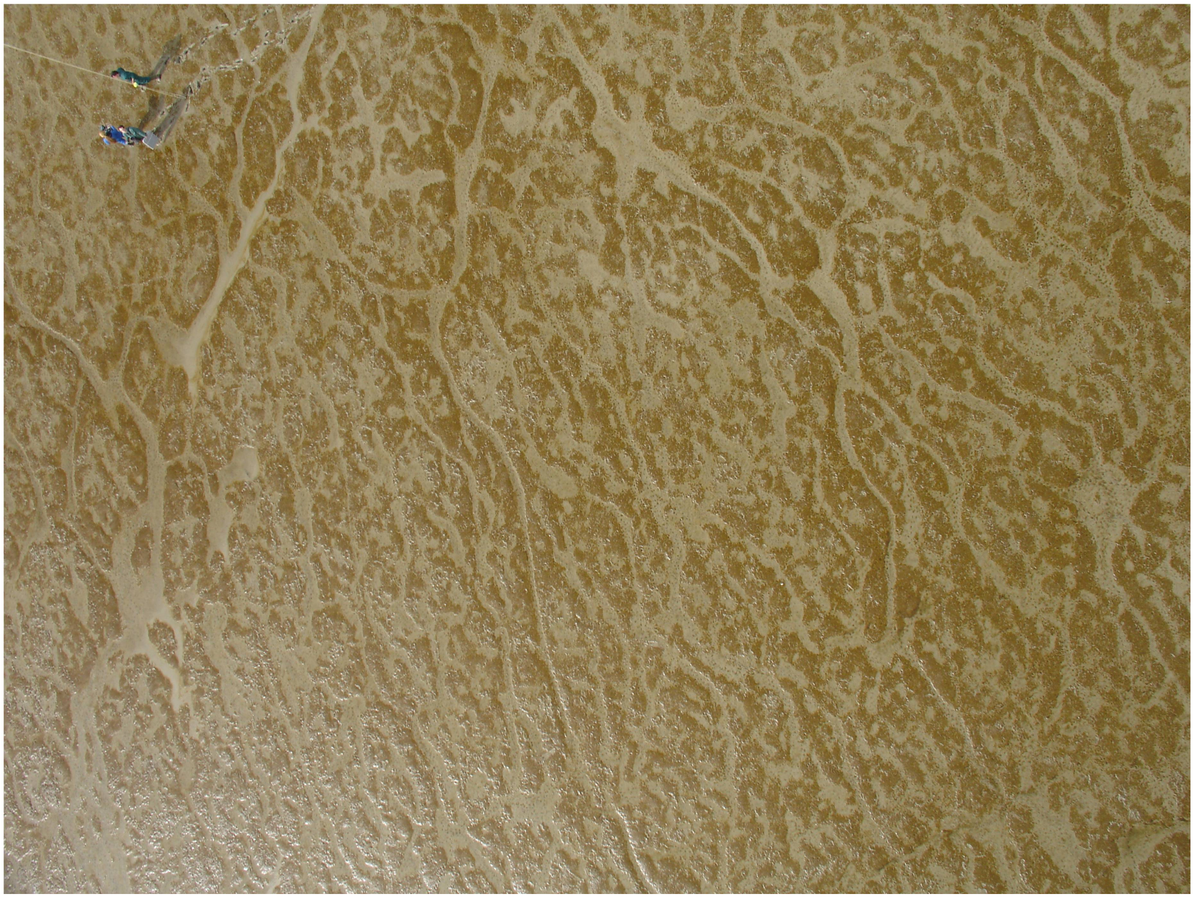

Figure B1: Aerial photograph taken for regularity analysis. Brown areas correspond to high diatom biomass, and gray areas correspond to almost bare sediment.

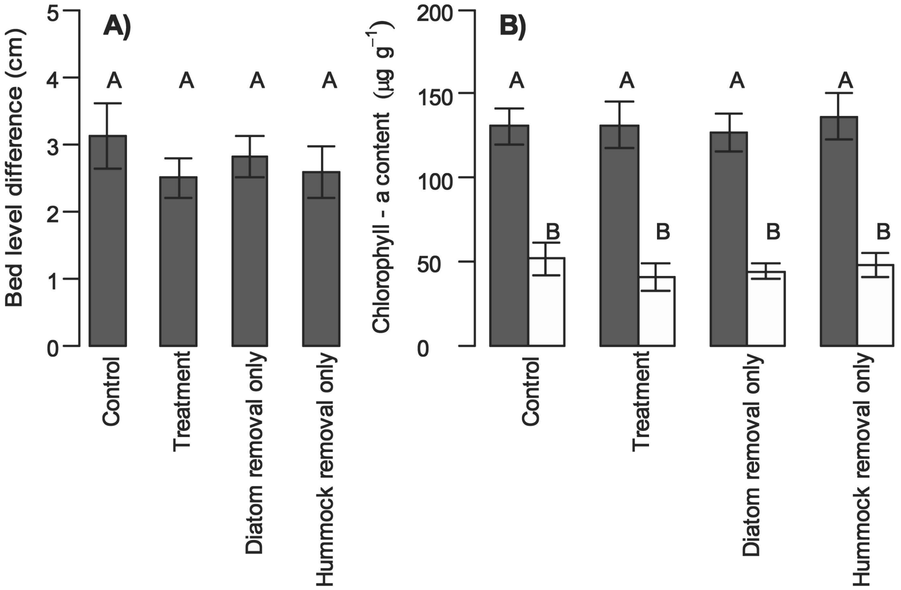

Figure B2: Bed level differences (*A*) and chlorophyll *a* content (*B*) of the different treatments after 14 days of treatment application. Gray bars in *B* represent hummocks, and white bars represent hollows ($n = 10$, standard bars denote SEM).

fects of removal of underlying heterogeneity on spatial pattern development.

Photograph Taken for Analysis of Spatial Patterns

Figure B1 is an example of an aerial photograph that was used for the regularity analysis (fig. 4). The photograph was taken from a blimp at about 50 m height; brown areas correspond to high diatom biomass patches, and gray colors correspond to almost bare sediment patches.

The Effects of the Removal of Underlying Physical Heterogeneity on the Formation of Spatial Patterns

To test the prediction that self-organized patterns could develop in the absence of underlying heterogeneity—for example, even on flat sediment—we removed variation in sediment elevation and diatom biomass.

Methods. On the Kapellebank tidal flat, we located 20 plots of 2 m × 2 m in sets of four. We collected the diatoms from the sediment surface using floor sweepers. The top layer of the sediment was then leveled, again using floor sweepers. The recovery of diatom biomass and patchiness within a 2-week period was compared with a control plot, where natural patterning was kept intact. To account for differential effects of diatom removal and sediment leveling, we added two procedural control treatments. In the first procedural control treatment, we removed only the diatoms. In the second, we initially removed diatoms, after which the sediment was leveled and diatoms were smeared back on top of the leveled sediment. All treatments were grouped and replicated five times over the entire intertidal flat following a randomized block design (Sokal and Rohlf 1995). We measured average diatom biomass and bed level differences after 14 days of treatment application. To account for changes in time, we replicated this whole experiment two times within a month. Repeated measurements during the experiment were not possible since entering the plots would disturb the buildup of the spatial structure. At each plot, chlorophyll *a* samples of the top 1 cm of the sediment were taken using a cut-off syringe (diameter 1 cm). In the laboratory, chlorophyll *a* samples were freeze-dried and analyzed spectrophotometrically after 48-h extraction in 90% acetone (Jeffrey and Humphrey 1975). Bed level differences were measured using a white board (0.85 m × 0.50 m) on which a grid was drawn that was placed vertically into the sediment in such a way that a hummock and a hollow were included in the pictures. Digital photographs of the grid board (about 2,560 pixels × 1,920 pixels) were geocorrected using Leica image processing software, following the procedure by van der Wal et al. (2005). Hummock development at each location was expressed as the difference between maximum and minimum bed level.

Statistical Analysis. The effect of the removal of underlying heterogeneity was determined using a univariate analysis with treatment and sample date as fixed factors and block as a covariate. Normal distribution of the data was checked by visual inspection of Q-Q plots, and Levene's test was used for testing homogeneity of variances.

Results. Treatment application was successful, since after 1 day patterns were still lacking on plots where patterns were removed (fig. B2*A*). Time and block did not have a significant effect on chlorophyll *a* content or bed level differences (ANOVA, $P < .05$). Therefore, all the data from different dates and blocks were pooled and analyzed for treatments effects 14 days after the treatment application. We found that for all treatments, the patterns had fully recovered. No differences were found in bed level between the control plots (3.12 ± 0.34 cm), treatment plots (2.50 ± 0.26 cm), and procedural controls (diatom removal only: 2.82 ± 0.28 cm; hummock removal only: 2.58 ± 0.34 cm; fig. B2*A*; $P > .05$). Similarly, no differences in chlorophyll *a* content were measured on hummocks between the control plots (133.1 ± 37.5 μg g^{-1}), treatment plots (133.1 ± 37.5 μg g^{-1}), and procedural controls (diatom removal: 124.6 ± 40.5 μg g^{-1}; hummock removal: 133.1 ± 37.5 μg g^{-1}) or in the hollows (control plots: 55.8 ± 19.3 μg g^{-1}; treatment plots: 38.0 ± 17.1 μg g^{-1}) and procedural controls (diatom removal: 46.6 ± 18.6 μg g^{-1}; hummock removal: 45.9 ± 11.6 μg g^{-1}; fig. B2*A*; $P < .05$).

Literature Cited Only in Appendixes A and B

Jeffrey, S. W., and G. F. Humphrey. 1975. New spectrophotometric equations for determining chlorophylls *a*, *b*, *c1* and *c2* in higher plants, algae and natural phytoplankton. Biochemie und Physiologie der Pflanzen 167:191–194.

Morris, E. P. 2005. Quantifying primary production of microphytobenthos: application of optical methods. PhD thesis. University of Groningen.

Tolhurst, T. J., K. S. Black, S. A. Shayler, S. Mather, I. Black, K. Baker, and D. M. Paterson. 1999. Measuring the in situ erosion shear stress of intertidal sediments with the cohesive strength meter (CSM). Estuarine, Coastal, and Shelf Science 49:281–294.

Tolhurst, T. J., K. S. Black, D. M. Paterson, H. J. Mitchener, G. R. Termaat, and S. A. Shayler. 2000. A comparison and measurement standardization of four in situ devices for determining the erosion shear stress of intertidal sediments. Continental Shelf Research 20: 1397–1418.

van der Wal, D., P. M. J. Herman, and A. Wielemaker-van den Dool. 2005. Characterisation of surface roughness and sediment texture of intertidal flats using ERS SAR imagery. Remote Sensing of Environment 98:96–109.

van Wijnen, H. J., and J. P. Bakker. 2001. Long-term surface elevation change in salt marshes: a prediction of marsh response to future sea-level rise. Estuarine, Coastal, and Shelf Science 52:381–390.

Wood, R., and J. Widdows. 2002. A model of sediment transport over an intertidal transect, comparing the influences of biological and physical factors. Limnology and Oceanography 47:848–855.

Literature Cited

Austen, I., T. J. Andersen, and K. Edelvang. 1999. The influence of benthic diatoms and invertebrates on the erodibility of an intertidal mudflat, the Danish Wadden Sea. Estuarine, Coastal, and Shelf Science 49:99–111.

Bassoullet, P., P. Le Hir, D. Gouleau, and S. Robert. 2000. Sediment transport over an intertidal mudflat: field investigations and estimation of fluxes within the "Baie de Marennes-Oleron" (France). Continental Shelf Research 20:1635–1653.

Blanchard, G. F., D. M. Paterson, L. J. Stal, P. Richard, R. Galois, V. Huet, J. Kelly, et al. 2000. The effect of geomorphological structures on potential biostabilisation by microphytobenthos on intertidal mudflats. Continental Shelf Research 20:1243–1256.

Borsje, B. W., M. B. de Vries, S. Huscher, and G. J. de Boer. 2008. Modeling large-scale cohesive sediment transport affected by small-scale biological activity. Estuarine, Coastal, and Shelf Science 78:468–480.

Champneys, A. R. 1996. Homoclinic orbits in reversible systems and their applications in mechanics, fluids and optics. Physica D 112: 158–186.

Couteron, P., and O. Lejeune. 2001. Periodic spotted patterns in semi-arid vegetation explained by a propagation-inhibition model. Journal of Ecology 89:616–628.

Crawley, M. J. 2005. The R book. Wiley, Chichester.

D'Alpaos, A., S. Lanzoni, M. Marani, and A. Rinaldo. 2007. Landscape evolution in tidal embayments: modeling the interplay of erosion, sedimentation, and vegetation dynamics. Journal of Geophysical Research 112:F01008.

de Boer, P. L. 1981. Mechanical effects of micro-organisms on intertidal bedform migration. Sedimentology 28:129–132.

de Brouwer, J. F. C., S. Bjelic, E. de Deckere, and L. J. Stal. 2000. Interplay between biology and sedimentology in a mudflat (Biezelingse Ham, Westerschelde, The Netherlands). Continental Shelf Research 20:1159–1177.

de Jonge, V. N., and J. E. E. van Beusekom. 1992. Contribution of resuspended microphytobenthos to total phytoplankton in the EMS estuary and its possible role for grazers. Netherlands Journal of Sea Research 30:91–105.

Doedel, E. J., R. C. Paffenroth, A. Champneys, T. F. Fairgrieve, Y. A. Kuznetsov, B. E. Oldman, B. Sandstede, and X. Wang. 2001. AUTO 2000: continuation and bifurcation software for ordinary differential equations (with HOMCONT). Technical report. Concordia University, Montreal. http://indy.cs.concordia.ca/auto/.

Eppinga, M. B., M. Rietkerk, W. Borren, E. D. Lapshina, W. Bleuten, and M. J. Wassen. 2008. Regular surface patterning of peatlands: confronting theory with field data. Ecosystems 11:520–536.

Gouleau, D., J. M. Jouanneau, O. Weber, and P. G. Sauriau. 2000. Short- and long-term sedimentation on Montportail-Brouage intertidal mudflat, Marennes-Oleron Bay (France). Continental Shelf Research 20:1513–1530.

Herman, P. M. J., J. J. Middelburg, J. Widdows, C. H. Lucas, and C. H. R. Heip. 2000. Stable isotopes' as trophic tracers: combining field sampling and manipulative labelling of food resources for macrobenthos. Marine Ecology Progress Series 204:79–92.

Herman, P. M. J., J. J. Middelburg, and C. H. R. Heip. 2001. Benthic community structure and sediment processes on an intertidal flat: results from the ECOFLAT project. Continental Shelf Research 21: 2055–2071.

Hiemstra, C. A., G. E. Liston, and W. A. Reiners. 2002. Snow redistribution by wind and interactions with vegetation at upper treeline in the Medicine Bow Mountains, Wyoming, USA. Arctic, Antarctic, and Alpine Research 34:262–273.

———. 2006. Observing, modelling, and validating snow redistribution by wind in a Wyoming upper treeline landscape. Ecological Modelling 197:35–51.

Knobloch, E. 2008. Spatially localized structures in dissipative systems: open problems. Nonlinearity 21:T45–T60.

Lanuru, M., R. Riethmuller, C. van Bernem, and K. Heymann. 2007. The effect of bedforms (crest and trough systems) on sediment erodibility on a back-barrier tidal flat of the East Frisian Wadden Sea, Germany. Estuarine, Coastal, and Shelf Science 72:603–614.

Larsen, L. G., J. W. Harvey, and J. P. Crimaldi. 2007. A delicate balance: ecohydrological feedbacks governing landscape morphology in a lotic peatland. Ecological Monographs 77:591–614.

Legendre, P., and L. Legendre. 1998. Numerical ecology. 2nd ed. Elsevier Science, Amsterdam.

Le Hir, P., W. Roberts, O. Cazaillet, M. Christie, P. Bassoullet, and C. Bacher. 2000. Characterization of intertidal flat hydrodynamics. Continental Shelf Research 20:1433–1459.

Le Hir, P., Y. Monbet, and F. Orvain. 2007. Sediment erodability in sediment transport modelling: can we account for biota effects? Continental Shelf Research 27:1116–1142.

Levin, S. A., and L. A. Segel. 1985. Pattern generation in space and aspect. SIAM Review 27:45–67.

Montserrat, F., C. Van Colen, S. Degraer, T. Ysebaert, and P. M. J. Herman. 2008. Benthic community-mediated sediment dynamics. Marine Ecology Progress Series 372:43–59.

Montserrat, F., C. Van Colen, P. Provoost, M. Milla, M. Ponti, K. Van den Meersche, T. Ysebaert, and P. M. J. Herman. 2009. Sediment segregation by biodiffusing bivalves. Estuarine, Coastal, and Shelf Science 83:379–391.

Neumann, A. C., C. D. Gebelein, and T. P. Scoffin. 1970. Composition, structure and erodability of subtidal mats, Abaco, Bahamas. Journal of Sedimentary Petrology 40:274–297.

Paarlberg, A. J., M. A. F. Knaapen, M. B. de Vries, S. Huscher, and Z. B. Wang. 2005. Biological influences on morphology and bed composition of an intertidal flat. Estuarine, Coastal, and Shelf Science 64:577–590.

Paterson, D. M. 1989. Short-term changes in the erodibility of intertidal cohesive sediments related to the migratory behavior of epipelic diatoms. Limnology and Oceanography 34:223–234.

Paterson, D. M., T. J. Tolhurst, J. A. Kelly, C. Honeywill, E. de Deckere, V. Huet, S. A. Shayler, K. S. Black, J. de Brouwer, and I. Davidson. 2000. Variations in sediment properties, Skeffling mudflat, Humber Estuary, UK. Continental Shelf Research 20:1373–1396.

Rietkerk, M., and J. van de Koppel. 2008. Regular pattern formation in real ecosystems. Trends in Ecology & Evolution 23:169–175.

Rietkerk, M., M. C. Boerlijst, F. van Langevelde, R. HilleRisLambers, J. van de Koppel, L. Kumar, H. H. T. Prins, and A. M. de Roos. 2002. Self-organization of vegetation in arid ecosystems. American Naturalist 160:524–530.

Rietkerk, M., S. C. Dekker, M. J. Wassen, A. W. M. Verkroost, and M. F. P. Bierkens. 2004*a*. A putative mechanism for bog patterning. American Naturalist 163:699–708.

Rietkerk, M., S. C. Dekker, P. C. de Ruiter, and J. van de Koppel. 2004*b*. Self-organized patchiness and catastrophic shifts in ecosystems. Science 305:1926–1929.

Saco, P. M., G. R. Willgoose, and G. R. Hancock. 2007. Eco-geomorphology of banded vegetation patterns in arid and semi-arid regions. Hydrology and Earth System Sciences 11:1717–1730.

Scheffer, M., and S. R. Carpenter. 2003. Catastrophic regime shifts in ecosystems: linking theory to observation. Trends in Ecology & Evolution 18:648–656.

Sherratt, J. A., and G. J. Lord. 2007. Nonlinear dynamics and pattern bifurcations in a model for vegetation stripes in semi-arid environments. Theoretical Population Biology 71:1–11.

Sokal, R. R., and F. J. Rohlf. 1995. Biometry: the principles and practice of statistics in biological research. 3rd ed. W. H. Freeman, New York.

Staats, N., E. de Deckere, B. Kornman, W. van der Lee, R. Termaat, J. Terwindt, and B. de Winder. 2001. Observations on suspended particulate matter (SPM) and microalgae in the Dollard Estuary, The Netherlands: importance of late winter ice cover of the intertidal flats. Estuarine, Coastal, and Shelf Science 53:297–306.

Stal, L. J. 2009. Microphytobenthos as a biogeomorphological force in intertidal sediment stabilization. Ecological Engineering 36:236–245, doi:10.1016/j.ecoleng.2008.12.032.

Stallins, J. A. 2006. Geomorphology and ecology: unifying themes for complex systems in biogeomorphology. Geomorphology 77: 207–216.

Sutherland, T. F., C. L. Amos, and J. Grant. 1998*a*. The effect of buoyant biofilms on the erodibility of sublittoral sediments of a temperate microtidal estuary. Limnology and Oceanography 43: 225–235.

Sutherland, T. F., J. Grant, and C. L. Amos. 1998*b*. The effect of carbohydrate production by the diatom *Nitzschia curvilineata* on the erodibility of sediment. Limnology and Oceanography 43:65–72.

Temmerman, S., T. J. Bouma, G. Govers, Z. B. Wang, M. B. De Vries, and P. M. J. Herman. 2005. Impact of vegetation on flow routing and sedimentation patterns: three-dimensional modeling for a tidal marsh. Journal of Geophysical Research 110:F04019.

Temmerman, S., T. J. Bouma, J. van de Koppel, D. D. Van der Wal, M. B. De Vries, and P. M. J. Herman. 2007. Vegetation causes channel erosion in a tidal landscape. Geology 35:631–634.

Underwood, G. J. C., and D. M. Paterson. 1993. Recovery of intertidal benthic diatoms after biocide treatment and associated sediment dynamics. Journal of the Marine Biological Association of the United Kingdom 73:25–45.

Underwood, G. J. C., C. Nilsson, K. Sundback, and A. Wulff. 1999. Short-term effects of UVB radiation on chlorophyll fluorescence, biomass, pigments, and carbohydrate fractions in a benthic diatom mat. Journal of Phycology 35:656–666.

van de Koppel, J., P. M. J. Herman, P. Thoolen, and C. H. R. Heip. 2001. Do alternate stable states occur in natural ecosystems? evidence from a tidal flat. Ecology 82:3449–3461.

van Oevelen, D., K. Soetaert, J. J. Middelburg, P. M. J. Herman, L. Moodley, I. Hamels, T. Moens, and C. H. R. Heip. 2006. Carbon flows through a benthic food web: integrating biomass, isotope and tracer data. Journal of Marine Research 64:453–482.

van Wesenbeeck, B. K., J. van de Koppel, P. M. J. Herman, and T. J. Bouma. 2008. Does scale-dependent feedback explain spatial complexity in salt-marsh ecosystems? Oikos 117:152–159.

Wang, R. H., Q. X. Liu, G. Q. Sun, Z. Jin, and J. van de Koppel. 2009. Nonlinear dynamic and pattern bifurcations in a model for spatial patterns in young mussel beds. Journal of the Royal Society Interface 6:705–718.

Whitehouse, R. J. S., P. Bassoullet, K. R. Dyer, H. J. Mitchener, and W. Roberts. 2000. The influence of bedforms on flow and sediment transport over intertidal mudflats. Continental Shelf Research 20: 1099–1124.

Williams, J. J., P. A. Carling, C. L. Amos, and C. Thompson. 2008. Field investigation of ridge-runnel dynamics on an intertidal mudflat. Estuarine, Coastal, and Shelf Science 79:213–229.

Winterwerp, J. C., and W. G. M. Van Kesteren. 2004. Introduction to the physics of cohesive sediment in the marine environment. Elsevier, Amsterdam.

Associate Editor: Christopher A. Klausmeier
Editor: Donald L. DeAngelis